Proceedings of the
7th Graz Brain-Computer Interface Conference 2017 DOI: 10.3217/978-3-85125-533-1-41

FEATURE EXTRACTION OF EVENT RELATED POTENTIAL BASED ON TIME AND FREQUENCY DOMAIN ANALYSIS

G. Kaur[1], N. K. Roma[1], B. Bhattacharya[1], P. Sircar[1]

[1]Indian Institute of Technology Kanpur, U.P., India

E-mail: gagank@iitk.ac.in

ABSTRACT: The event related potential is traditionally obtained in time domain by computing ensemble average. However, due to non-stationarity and poor localization of these signals, this may result in erroneous feature extraction. In this present study, a standard database is considered to elucidate this problem. It is shown that a frequency domain decomposition followed by the estimation of spectral distance by measures like Itakura-Saito distance may partially resolve the problem. However, recognizing the contribution of endogenous and exogenous inputs to each event related potential, it is further argued that a Wavelet Packet Decomposition may be more useful since each signal in the frequency domain can be further decomposed into five characteristic domains (delta, theta, alpha, beta, and gamma) and based on the feasibility of contributions from each domain a better feature extraction will be possible.

INTRODUCTION

Oddball paradigm is an experimental standard used in several studies to elicit event related potential (ERP) and analyze its subcomponents. In this paradigm, a visual stimulus is presented where a sequence of random elements are displayed with a high likelihood (80-90%), non-target stimuli and is interjected by a low likelihood (5-20%), the "oddball" stimuli, which might vary in duration and intensity [1].

The salience associated with stimulus ensures the occurrence of P300; more the event has an element of surprise to it, stronger is the response. Hence the stimulus should be designed in such a way that the desired event be randomly positioned and infrequently presented among a series of non-target events. The present study focuses on an enhanced component of ERP, the P3b observed at the parietal region; commonly known as the P300. It occurs around 300ms +/- 100ms after the onset of target stimulus. The amplitude of P300 varies directly with the relevance of the eliciting events and inversely with the probability of the stimuli [2].

The ERP waveform has the observable peaks and troughs; however, it has also the unobservable latent components. It is these latent components that give measure of neuronal response to visual stimulation task, the peaks are a summation of latent components. The latency, amplitude and duration of latent components vary across trials. Once the ensemble averaging over multiple trials is done, nothing can be ascertained about the behaviour of these components.Given this, latency and amplitude may not be sufficient measures to compare two ERPs [3].Additionally,ERP phase can also shift across trials,which would imply, that the signal to noise ratio will deteriorate after ensemble averaging. Using the well-known time-frequency inverse relation; it is hypothesized that a large shift in time latency will depict as a small variation in the frequency of ERP component. Thus, irrespective of shift in phase; using frequency as the feature could determine presence of P3b-ERP. To further argue the choice of frequency as a probable feature in a practical system, one may assume a small window of samples taken after each run. Within this window the amplitude and phase are non-deterministic whereas frequency is a deterministic parameter.While state of the art algorithms are well equipped to analyze deterministic signals, it is still challenging to investigate the non-deterministic signals.For some time, wavelet transforms have been used to observe ERPs by choosing appropriate mother wavelets and manipulation of bases functions gives a closer look at the wave shapes. This approach helps with choice of filters to be used, extraction of single trial ERP, breaking down ERP response into various frequency bands, detection of overlapping peaks[4]. [5] Another study discusses which single channel wavelet transform to auditory evoked potentials in cats. It also draws attention to limitations of sole reliance on amplitude and latency and highlights ability of wavelet transform to identify ERP components and effects of various experimental conditions on properties of these components. [6]This study used simulated EEG data generated using Gabor logons and chirped signals. To extract P300, time frequency transformation using morlet wavelet and reduced interference distribution (RID) are fed as inputs to principal component analysis (PCA). It reduced three dimensional data to two dimensional vectors which further retrieved P300 ERP. Wavelet analysis indicated that appreciable theta activity was related to the more novel non-target stimuli; primarily target component delta coefficients were affected by the discrimination difficulty variable. In the present study, it is proposed that a frequency domain analysis be followed after the time domain ensemble averaging. Further the ERP be decomposed and visualized in terms of basic brain rhythms using wavelet packet decomposition.

 DOI: 10.3217/978-3-85125-533-1-41

MATERIALS AND METHODS

The present study uses P300 speller dataset from BCI competition III webpage with due acknowledgement [7].In the beginning, an ensemble average of a single trial, corresponding to a target is obtained; the spectral components of the signal are extracted, using DFT.Following this, the spectral components of all ensuing trials are computed. Subsequently, using some of the spectral distance measure techniques, the spectral distances between the initial trial and each of the subsequent trials are computed. It is assumed that if a threshold for each of these spectral distances is selected, and then target and non-target may be differentiated.

The input EEG signal is sampled at 240Hz.There are 85 epochs, each having a target character. Also an epoch contains 7794 samples, but for the purpose of ERP retrieval, individual trails are extracted from within each epoch. Each trial has 240 samples. The process of extracting samples from epochs can potentially corrupt the original signal by introducing noise. To avoid this, appropriate window functions are applied to the signal while deducting samples. Windows are selected so that the signal smoothly approaches zero at both ends.

The fast Fourier transform algorithm has been be used for ensemble average of each trial, i.e. 240 samples taken over 1000ms while DFT is designed for signal extending from 0 to ∞. For such a case, nothing can be known about the signal behavior outside the measured interval and the Fourier transform makes an implicit assumption; that the signal is repetitive. This assumption leads to discontinuities that are not really present in signal. Since sharp discontinuities have broad frequency spectra, this will cause frequency spectra to spread out. Consequently, the signal energy which should be concentrated only at one frequency instead leaks into other frequencies. This will lower the signal to noise ratio. Secondly, the spectral leakage from a large signal component may be severe enough to mask other smaller signals at different frequencies.

Thus, the signal is multiplied within the measurement-time, by some function that smoothly reduces the signal to zero at the end points; hence, avoiding the discontinuities altogether and curtailing the spectral leakage. Further it is expected to reduce the contribution of each frequency to one DFT bin.

The basic discrete Fourier transform (DFT) synthesis and analysis equations are

$$X[k] = \sum_{n=0}^{N-1} x[n] e^{jk\Omega_o n}, 0 \leq k \leq N-1 \qquad (1)$$

$$x[n] = \frac{1}{N} \sum_{k=0}^{N-1} X[k] e^{-jk\Omega_o n}, 0 \leq n \leq N-1 \qquad (2)$$

$X[k]$ and $x[n]$ are periodic sequences in frequency and time domains respectively. $X[k]$ is equal to samples of periodic fourier transform $X(e^{j\omega})$. $X[k]$ will be the transform of a periodic extension of $x[n]$ for n outside the interval $0 \leq n \leq N-1$. In defining DFT representation, we are recognizing that we are interested in values of $x[n]$ only in the interval $0 \leq n \leq N-1$ because $x[n]$ is really zero outside this interval. k represents discrete instances in frequency, n represents the number of samples in time, N the period, j represents $\sqrt{-1}$, Ω_o represents discrete frequency [8].

Distance measure is a common technique used to measure difference between a model/estimate(s) and its observations.The spectral distances are computed using second order properties of signal. Current study uses asymmetric and symmetric distance measures to gauge target and non-target ERP responses.

The Itakura-saito distance measure is defined as

$$D_{IS}(P(w_k), \widehat{P}(w_k)) = \frac{1}{N} \sum_{k=0}^{N-1} \frac{|X[k]|^2}{\left|\widehat{X}[k]\right|^2} - \frac{1}{N} \sum_{k=0}^{N-1} \left[\log \frac{|X[k]|^2}{\left|\widehat{X}[k]\right|^2} - 1 \right] \qquad (3)$$

where $k = 0, 1, ..., N-1$ and $P(w_k) = |X[k]|^2$

It is a measure of difference between original spectrum (template P300 in present context) $P(w)$ and a typical observation that can be considered as an approximation $\widehat{P}(w)$ of that spectrum. It is intended to reflect structural dissimilarity. Further Itakura-Saito distance is a Bregman divergence which is not a true metric since it fails to meet the symmetry and inequality axioms.

Spectral distances between two spectral densities $P(w_m)$ and $\widehat{P}(w_m)$ can be measured using L_q norm of the difference between them, depicted as;

$$D(P(w_m), \widehat{P}(w_m)) = \left\| P(w_m) - \widehat{P}(w_m) \right\|_q \qquad (4)$$

Such distances satisfy triangular inequality and symmetry property and are thus true distances [9].

A spectral distance measure D can be symmetrized by extending D_{IS} as shown:

$$D_{cosh} = \frac{1}{N} \sum_{m=1}^{N} \left[\frac{P(w_m)}{\widehat{P}(w_m)} - \log \frac{P(w_m)}{\widehat{P}(w_m)} + \frac{\widehat{P}(w_m)}{P(w_m)} \right] - \frac{1}{N} \sum_{m=1}^{N} \left[\log \frac{\widehat{P}(w_m)}{P(w_m)} - 2 \right] \qquad (5)$$

One of the main spectral deviation measures is log spectral, defined by L_q norm of difference between log of spectra $D = \left\| \log \frac{P(w_m)}{\widehat{P}(w_m)} \right\|_q$ where $q = 2$ for root mean square (rms) or the mean quadratic distance given below:

$$D_{rms} = \frac{1}{2N} \sum_{m=1}^{N} \left[\log \frac{P(w_m)}{\widehat{P}(w_m)} \right]^2 \qquad (6)$$

 DOI: 10.3217/978-3-85125-533-1-41

Given a signal, the wavelet packet decomposition filters the signal into equal low-frequency and high-frequency subspaces. Present study uses MATLAB software for wavelet packet decomposition. Averaged trials from individual epochs were the input signals and decomposition into the lower frequencies was repeated till level 5. Daubechies wavelet of order 8 was used as the mother wavelet. The outcome was signals divided into delta, theta, alpha, beta, gamma activity.

RESULTS AND DISCUSSION

Ensemble averaging is one of the most popular time domain methods for extraction of ERP signatures. During the course of present investigation, it was found that this signature makes significant departure from its known pattern across trials. Fig. 1-3,are manifestations of the same. Fig. 1-3 are time domain ensemble average of target and non-target responses at frontal (Fz), Parietal (Pz) and occipital (Oz) electrodes, taken over duration of one second. In Figures 1 and 2, the target responses peaks at nearly 450 ms though the peaks begin to appear around 200 ms, modulated by a higher frequency noise. Both patterns closely match upto an expected ERP. It has to be noted though that they are not same, because, while what appeared at Pz correspond to P3b component, the response to rare target, in an oddball paradigm. The response at Fz is directing to P3a component which corresponds to non-target [10]. This distinction is important to make, in order to choose the right channel for analysis.

A marked departure from the said pattern can be seen in Fig. 3, which is a time domain ensemble average of target responses computed over central midline at the occipital lobe. Contrary to the norm, there is rather a dip spreading across 250-380 ms. One possible explanation could be that the ERP response is getting superimposed by a more prominent activity at the occipital lobe [11]. It is imperative to recognize the patterns associated with non-target responses. Ideally a non-target stimulus does not elicit the endogenous ERP component, specifically peak around 300ms. For example, the non-target in Figures 1 and 2 depicts compliance to the rule, while in Fig. 3, it does not. An small unanticipated peak appears between 300-400ms. A classifier such as PCA which is not able to handle jitters will not be able to make the system very much efficient with such responses in given signal. The present study proposes to compute spectral distances between two spectra. One is a fixed spectrum, that of a template or estimated ERP. The other is a dynamic spectrum which changes with each trial; in other words, spectrum of each subsequent trials. Itakura-Saito reveals the spectral distances between the two. The procedure to compute Itakura-Saito distance is as follows: 1- The first input is estimated and its spectrum is computed as follows: The grand average of responses to target stimuli for a single channel is taken.

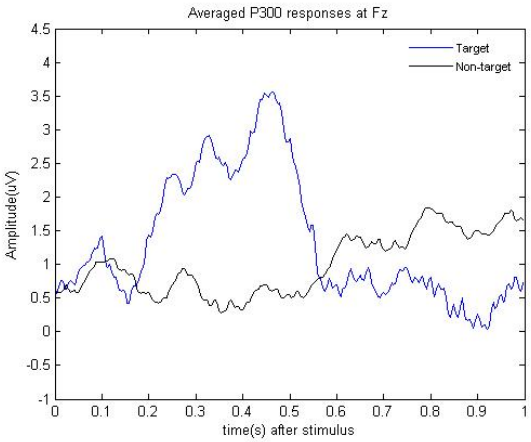

Figure 1: Target(T) and Non-Target(NT) responses at Fz.

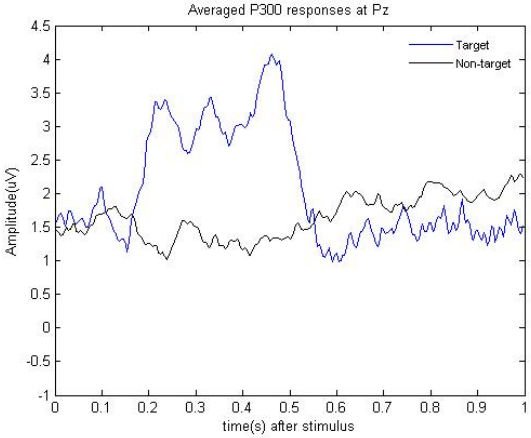

Figure 2: Target(T) and Non-Target(NT) responses at Pz.

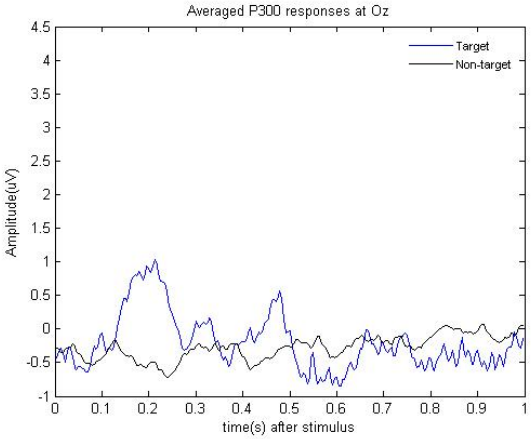

Figure 3: Target(T) and Non-Target(NT) responses at Oz.

To avoid high frequency noise modulation an appropriate window function is applied right before it is mapped onto the frequency domain using DFT. The spectral components thus retrieved are considered as desired markers of an ERP.

 DOI: 10.3217/978-3-85125-533-1-41

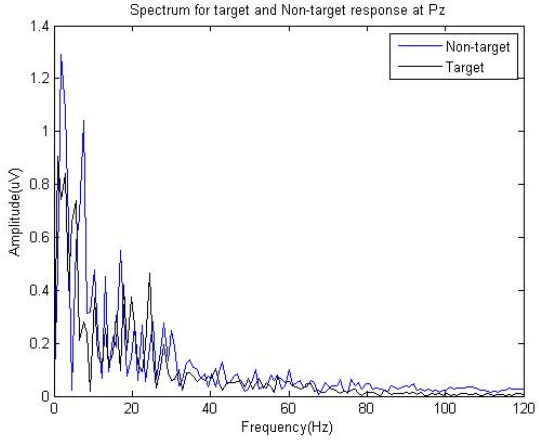

Figure 4a Frequency spectrum for target and non-target responses at Pz.

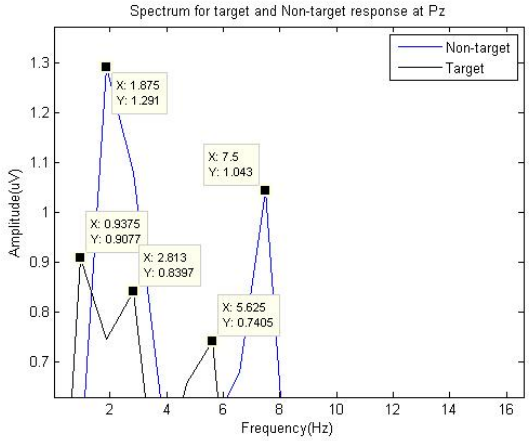

Fig 4b Closer look at frequency spectrum for target and non-target responses at Pz.

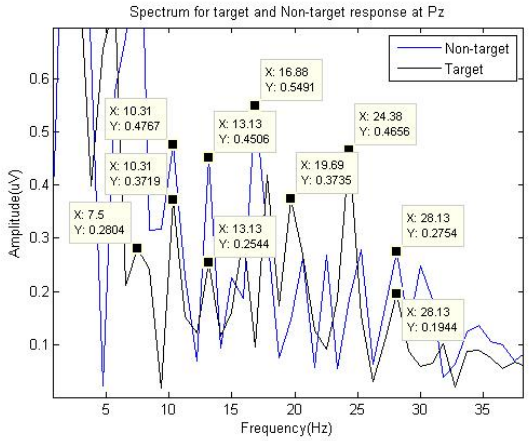

Fig 4c Closer look at frequency spectrum for target and non-target responses at Pz.

2- The template evaluated in earlier step is compared with respect to spectral components of each subsequent trial. These spectral components are computed in a similar fashion as described in the above step.

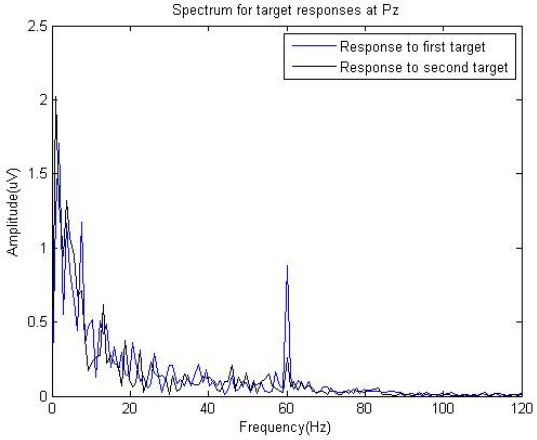

Figure 5a: Frequency spectrum for two target responses at Pz.

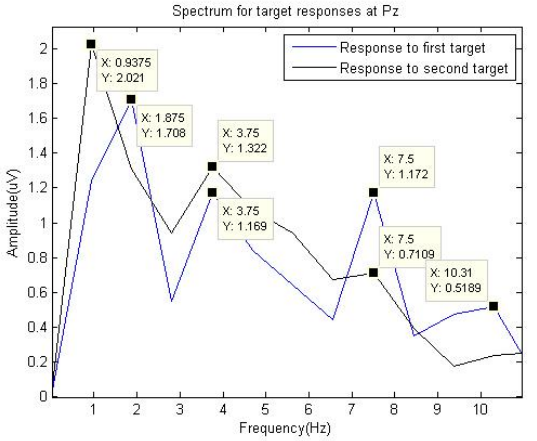

Figure 5b: Closer look at frequency spectrum for two target responses at Pz.

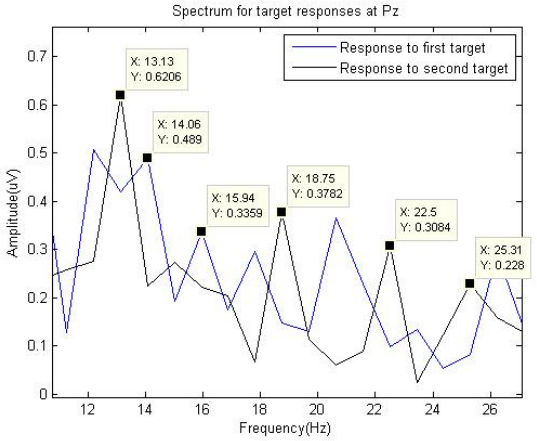

Figure 5c: Closer look at frequency spectrum for two target responses at Pz.

3- The Power spectra for estimated spectra as well as of individual trials are computed to evaluate the Itakura-Saito distance as described in equation (3). The Itakura-Saito distances was measured between, a target and a non-target, as well as, between two targets and following interesting observation were made. Ideally the frequency components while attending to the target and non-target

 DOI: 10.3217/978-3-85125-533-1-41

stimulus should differ, as attention to a target stimulus should elicit ERP response containing peak component at 300ms after stimulus onset. It was observed that both target and non-target responses had overlapping frequency components, to a certain degree Figures 4,5. Frequency spectrum of target responses between two trials is shown in Fig.5a-c, again while some components are overlapping; a disparity can also be observed. It can be explained by going back to jitter effects between trials in time domain.

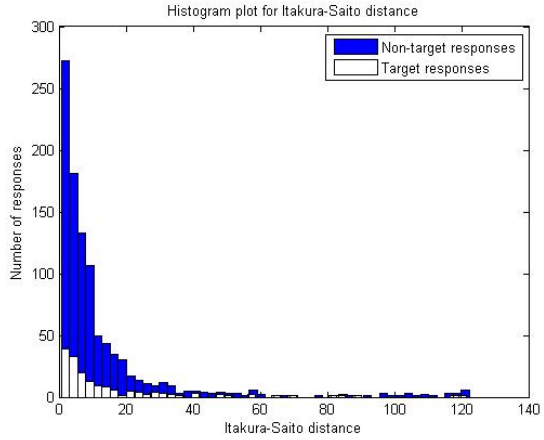

Figure 6: Itakura-Saito distance measure between the response corresponding to target stimuli and the non-target stimuli.

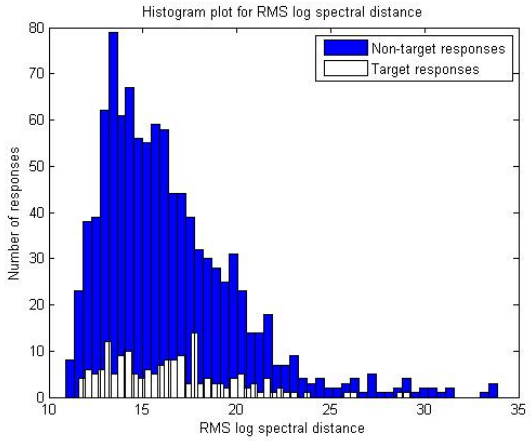

Figure 7: RMS Log Spectral distance measure between the response corresponding to target stimuli and the non-target stimuli.

Given the non-stationary nature of EEG signals, and presence of both endogenous and exogenous components in the ERP response these manifestations are hard to deal with by a simple mapping from time to frequency domain. This ambiguity calls for a more specific decomposition of the ERP. The overlap in frequency components of both targets and non-targets demands that the endogenous component, which is unique to target response be separated.

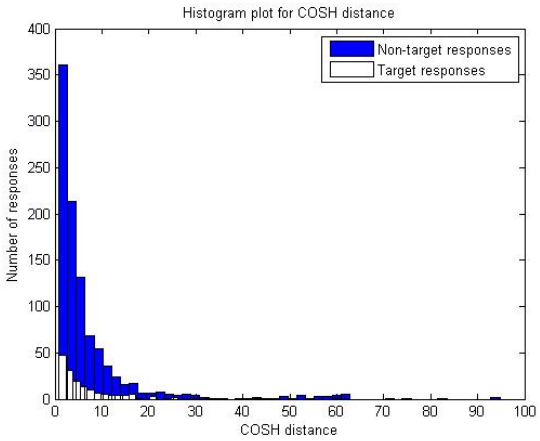

Figure 8: COSH distance measure between the response corresponding to target stimuli and the non-target stimuli.

In order to achieve this, wavelet packet decomposition (WPD) could be carried out, using an appropriate basis function. This shall be explained later in this section. If a standard pattern manifests every time an ERP is elicited, a measurement of spectral distance between a template target spectrum and response of subsequent ERP trials will be able to classify between target and non-target. Fig. 6-8 illustrate spectral distance measures between targets and non-targets for which, Pz channel is selected. At first, an asymmetric spectral distance measure is computed using Itakura-Saito distance. This distance is calculated between estimated spectrum and individual trials. The range of Itakura–Saito distance lies within 0-120 units which are divided in 50 bins. 87.5% of Nontarget and 81.1% of target responses falls within 0-25 units. This shows that high percent of both target and non-target stimuli lie in the same range and hence results in poor detection of target responses. It also depicts the generalization of our said observation for Fig. 4 and 5 across all trials. As the detection of target responses in Itakura-Saito became intricate, symmetric spectral distance measures were attempted. Here, RMS log spectral and COSH spectral distances were computed and their outcomes are shown in Fig. 7 and 8. In Fig. 7, RMS log spectral distance varies between 11- 22 units which is divided into 50 bins. 92.5% of nontarget and 94.7% of target stimuli falls within above range. It is observed that the responses are broadly distributed over a large range of distance. In Fig. 8, 91.5% of non-target and 88.2% of target responses are between 0-20 units of COSH distances. Consequently, the differentiation of target stimuli from non-target becomes obscure in both symmetric as well as asymmetric spectral distance measure methods. At this juncture, instead of looking at the ERP as a whole, wavelet packet decomposition was used to separate the ERP to lower frequency bands. After wavelet packets decomposition, an ERP could be visualized in terms of delta, theta, alpha, and beta rhythms. Fig. 9 shows decomposition of target and non-target activity at Pz.

 DOI: 10.3217/978-3-85125-533-1-41

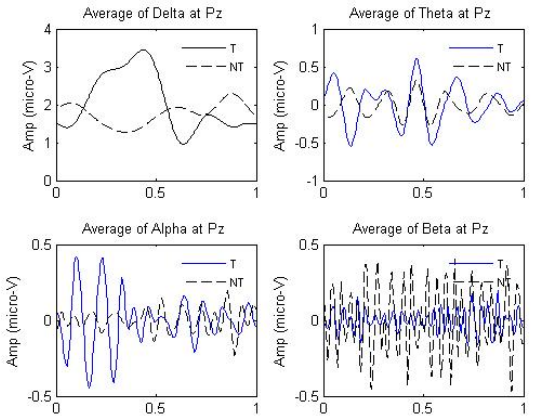

Figure 9: Average Delta, Theta, Alpha and Beta activities at Pz, corresponding to Target(T) and Non-Target(NT) responses.

As ERP is not a single response but rather a coagulation of exogenous and endogenous responses to the visual stimulation; coming from a highly non-linear system, the human brain. Decomposing ERP into multiple frequency bands rather than visualizing it as a whole shall be more befitting approach, to extract the endogenous P3b response to target stimuli.In present work when target and non-target responses were decomposed into multiple frequency bands using wavelet packet decomposition, Fig. 9. The delta rhythm associated with target has higher amplitude than for non-target. Theta activity is known to increase with increasing memory load; a slightly higher theta activity was observed for target responses. Alpha activity for target stimulus had higher amplitude compared to non-target when observed at Pz. The alpha activity is associated with idle state of brain region under consideration. But this statement would be an oversimplification given the fact that, different areas of brain possess their unique alpha activity. Parietal alpha power is known to increase as task load increases. There is a marked difference between beta activity of target and non-target. Such can be considered as a feature which can be used for classification between targets and non-targets. By keeping these results as basis, we will continue to take on a more thorough investigation on ERP components and identify more features for robust target classification.

CONCLUSION

The present study summoned up the non-stationary nature of event related potentials. On that premise, a scrutiny of common approaches for extraction of event related potentials from raw EEG data was instigated. The limitations of those approaches were accounted and the study proceeded to computation of spectral distance measures expecting to mark distinction between target and non-target ERP responses.

ACKNOWLEDGEMENTS

This work used BCI competition-III dataset provided by Wadsworth Center, NYS Department of Health (Jonathan R. Wolpaw, Gerwin Schalk, Dean Krusienski). The authors are thankful to Professor K.S. Venkatesh for providing time, space and resources for discussions and critical reviews.

REFERENCES

[1] Pfurtscheller G, Lopes da Silva FH. Handbook of Electroencephalography and Clinical Neurophysiology – Event-related desynchronization, Elsevier, Amsterdam, Netherlands (1999).Steven J. Luck, An Introduction to the Event-Related Potential Technique, Massachusetts Institute of Technology (2005).

[2] Neal R. Swerdlow (Ed.), Behavioral Neurobiology of Schizophrenia and Its Treatment. Springer-Verlag Berlin Heidelberg, April 2010 pp. 287.

[3] Luck, S. J. Ten Simple Rules for Designing and Interpreting ERP Experiments. In: Handy, TC (Ed.) Event-Related Potentials: A Methods Handbook.(2004), pp.20-30.

[4] Samar VJ, Swartz KP, Raghuveer MR. Multiresolution analysis of event-related potentials by wavelet decomposition. Brain and cognition. 1995 Apr 30;27(3):398-438.

[5] Raz J, Dickerson L, Turetsky B. A wavelet packet model of evoked potentials. Brain and Language. 1999 Jan 31;66(1):61-88.

[6] Bernat EM, Williams WJ, Gehring WJ. Decomposing ERP time–frequency energy using PCA. Clinical Neurophysiology. 2005;116(6):1314-34.

[7] G.Schalk, Dean Krusienski, 'BCI Competition III Challenge 2004', Wadsworth BCI Dataset (P300 Evoked Potentials), Data Acquired Using BCI2000's P3 Speller Paradigm.

[8] Alan V. Oppenheim and Ronald W. Schafer. The discrete Fourier Transform. In:Discrete-Time Signal Processing (3rd ed.). Prentice Hall Press, Upper Saddle River, NJ, USA, 2009, pp.669.

[9] Basseville M., Distance measures for signal processing and pattern recognition. Signal Processing. 1989 Dec 1;18(4):349-69.

[10] Polich J. Updating P300: an integrative theory of P3a and P3b. Clinical Neurophysiology. 2007 Oct 31;118(10):2128-48.

[11] Juri D. Kropotov, Beta Rhythms. In: Kropotov JD.Quantitative EEG, event-related potentials and neurotherapy. Academic Press; 2010 Jul 28.